American Mineralogist, Volume 84, pages 1512–1520, 1999

Determination of the influence of pressure and dissolved water on the viscosity of highly viscous melts: Application of a new parallel-plate viscometer

FRANK SCHULZE, HARALD BEHRENS, AND WILLY HURKUCK

Institut für Mineralogie, Universität Hannover, Welfengarten 1, D-30167 Hannover, Germany

ABSTRACT

A parallel-plate viscometer has been designed for use in an internally heated pressure vessel (IHPV) at pressures up to 350 MPa and at temperatures up to 900 °C. The viscosity of a melt is determined by measuring the rate of deformation of a cylindrical sample as a function of an applied, constant stress at a fixed temperature. The viscometer consists of a small furnace with two independent heating resistors, a moveable load by which the stress is applied to the sample, and a pressure-resistant transducer (LVDT) that measures the deformation of the sample. The accessible viscosity range covers three orders of magnitude from $10^{8.5}$ Pa·s to $10^{11.5}$ Pa·s.

Calibration measurements on the standard melt DGG1 at 0.1MPa demonstrated the precision of the viscometer to be within ±0.08 log units. Subsequent measurements at elevated pressure on DGG1-melt, Di_{100}-melt (Di = $CaMgSi_2O_6$), and $Ab_{55}Di_{45}$-melt (Ab = $NaAlSi_3O_8$, composition in weight percent) showed a pronounced increase of viscosity with pressure. Comparison with literature data on the pressure dependence of the transformation temperature of Di_{100}-melt (Rosenhauer et al. 1979) confirmed the reliability of these findings. The dependence on pressure becomes smaller with increasing temperature for these depolymerized melts; e.g., in the case of Di_{100}-melt (NBO/T = 2) from $d\eta/dP$ = +0.23 log units/100 MPa at 751 °C to $d\eta/dP$ = +0.18 log units/100 MPa at 770 °C. In contrast to the depolymerized melts, a polymerized melt of haplotonalitic composition (NBO/T = 0) shows a decrease by –0.12 log units/100 MPa in the pressure range 50–350 MPa at 889 °C.

Possible application of the new viscometer to study rheological properties of volatile-bearing melts was tested successfully with a hydrous haplotonalitic melt. Addition of 3.80 wt% of water to the anhydrous melt strongly shifts the viscosity-temperature relationship toward lower temperatures; e.g., at a viscosity of $10^{10.5}$ Pa·s from 883 to 515 °C. The measured viscosities did not drift during the run, indicating that water loss is negligible within the time scale of the experiments, as confirmed by IR-microspectroscopic analysis.

INTRODUCTION

In recent decades, considerable effort has been made to determine the viscosities of volatile-bearing, and especially hydrous melts, over a wide temperature range at geologically relevant pressures (e.g., Shaw 1963; Kushiro 1978; Dingwell and Mysen 1985; Dingwell 1987; Persikov et al. 1990; White and Montana 1990; Baker and Vaillancourt 1995; Schulze et al. 1996; Scaillet et al. 1996). The first data for water-bearing melts were obtained using the falling sphere technique (Shaw 1963). This method allows only a small viscosity range to be investigated (10^2 to 10^5 Pa·s), which is not always relevant to natural conditions (e.g., temperatures are too high for silica-rich melts). Furthermore, in the case of hydrous melts, the precision of the falling sphere technique is affected not only by serious experimental difficulties (Holtz et al. 1999) but also by poorly constrained melt densities at high *P* and *T*.

The extrapolation of viscosity data to lower temperatures has been hampered by the fact that up to now no generalized model existed to predict the temperature dependence of the viscosity of water-bearing melts. The widely used Arrhenius law (e.g., Shaw 1972; Persikov et al. 1990) fails to describe the temperature dependence of the viscosity of most silicate melts over a large temperature-range due to significant deviations from linearity (e.g., Richet and Bottinga 1995). Without measurements at lower temperatures and high pressure, the temperature dependence of viscosity due to the influence of pressure, as well as the influence of volatiles on the rheology of magmas, are poorly constrained.

One possibility for extending the viscosity range measurable by the falling sphere method was presented by Dorfmann et al. (1996) and Dorfmann et al. (1997). Using a centrifuge, viscosities up to 10^8 Pa·s can be determined at a confining pressure of up to 100 MPa. However, the usefulness of this technique is probably limited, because for many melts of geological relevance, problems can arise due to crystallization on the time scale of the experiment.

Another approach to determine the viscosity of highly viscous, water-bearing melts involves measurements at ambient pressure using experimental techniques developed for anhydrous melts (micro-penetration, Dingwell et al. 1996, 1998;

*E-mail: schulze@mineralogie.uni-hannover.de

0003-004X/99/0010–1512$05.00

creep deformation, Richet et al. 1996). It should be emphasized that these techniques are limited to relatively low water contents. At high water contents, water loss by diffusion and foaming of the samples becomes a major problem. Moreover, effects of pressure cannot be investigated.

In this study, we present a new parallel-plate viscometer developed to work in an internally heated pressure vessel (IHPV) under isostatic pressures up to 350 MPa and at temperatures up to 900 °C. The range of viscosities that could be measured with this setup is $10^{8.5}$ to $10^{11.5}$ Pa·s. Within this viscosity range, crystallization is of minor importance on the time scale of the experiments. The precision of the device has been tested using a viscosity standard glass as well as selected melts of geological relevance. First results on the pressure dependence of the viscosity of some anhydrous melts are presented. Thereafter, possible application of the new technique to the study of hydrous melts is discussed.

DESCRIPTION OF THE PARALLEL PLATE VISCOMETER

With the parallel plate viscometer developed in this study, the viscosity of a melt is determined by measuring the rate of deformation of a cylindrical sample of length l as a function of an applied constant stress σ at a fixed temperature. By noting the time t, the viscosity η of the sample is given by (Neuville and Richet 1991):

$$\eta = \frac{\sigma}{3 \cdot (\mathrm{d}\ln l \cdot \mathrm{d}t)} \quad (1)$$

The viscometer is designed to operate in a vertical, internally heated pressure vessel (IHPV) at pressures up to 350 MPa using Ar as the pressure medium. A large volume of 426 cm^3 (l = 28 cm, ∅ = 4.4 cm) is available in the IHPV to incorporate the various components of the experimental setup. A sketch of the viscometer is shown in Figure 1. The lower closure head of the IHPV holds the furnace and a device to apply the stress to the sample whereas the upper closure head holds a transducer to monitor the deformation rate of the sample.

Five ports are available in the lower closure head. Two of them are used for the power supply of the furnace and are sealed by steel cones insulated with Kynar heat-shrink sleeving. The other three ports are used for the thermocouple wires, which are made from thin, fiberglass insulated Ni or NiCr (∅ = 0.2 mm). The wires are passed through the ports in a thin layer of an Araldite/pyrophyllite mixture cast around a steel cone. Within the autoclave, the wires are connected to a small glass-epoxy printed circuit board mounted on the closure head. The type-K thermocouple wires connected to the circuit board are isolated by sintered, double-hole, alumina capillaries. The furnace of the viscometer, which is mounted on the lower closure head, consists of two heating zones made of Kanthal A1 wires (∅ = 0.6 mm) wound around a tube of sintered alumina (∅ = 15 mm). Both heating zones are controlled independently by a programmable temperature controller (Eurotherm 906 EPC). The use of two heating zones greatly reduces temperature gradients along the sample.

Both ends of the furnace are closed with steel plates. Two silica-glass pistons are guided into the furnace through bores in the plates. The lower piston is mounted on the closure head and extends into the hot zone of the furnace. The gap between the glass piston and the steel plate is sealed with Teflon tape to reduce convective flow of the pressure medium between the cold and the hot part of the viscometer. At the upper end of the silica piston a tube made of Ag is attached (length = 35 mm, i.d. = 8 mm, o.d. = 10 mm). This tube encloses the sample chamber and further reduces temperature gradients along the sample due to the high thermal conductivity of Ag. An enlarged

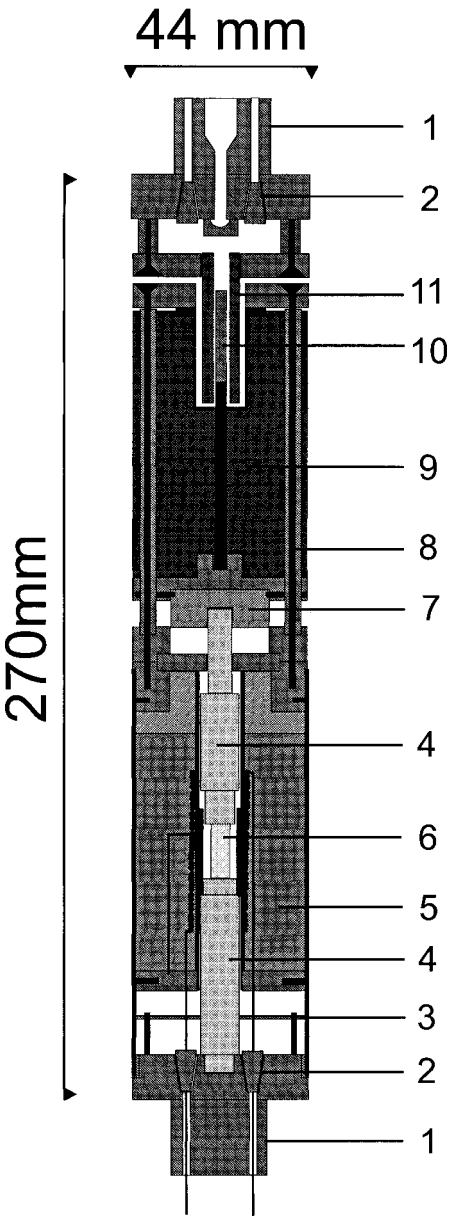

FIGURE 1. Schematic illustration of the parallel-plate viscometer: (1) closure head; (2) steel cone; (3) glass-epoxy printed circuit board; (4) silica-glass piston; (5) furnace; (6) sample; (7) ceramic shield; (8) guide bars; (9) load; (10) soft iron core; and (11) linear variable differential transducer. Thermocouples are not drawn in for clarity but are shown in the detailed illustration of the sample position (see Fig. 2)

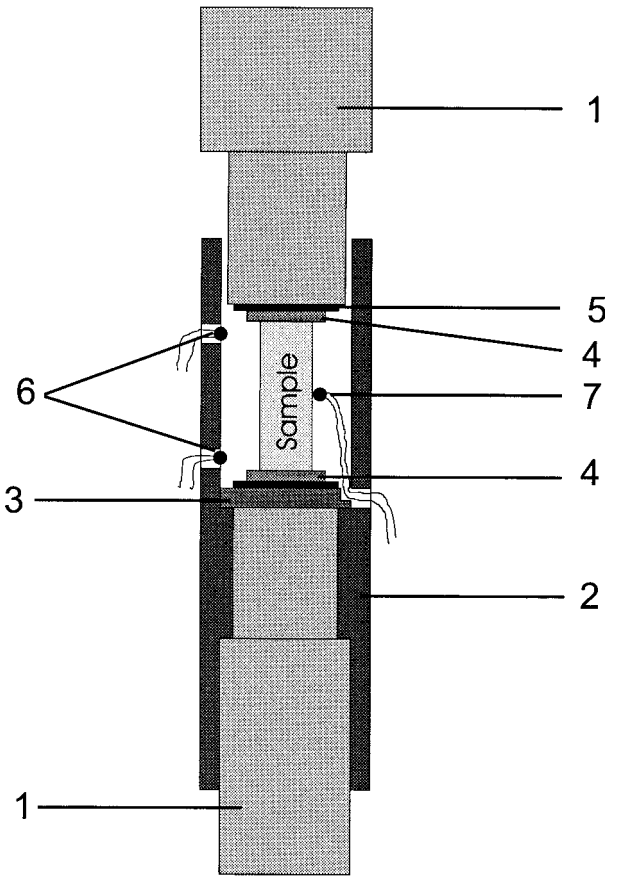

FIGURE 2. Details of the sample position: (1) silica-glass piston; (2) Ag tube; (3) ceramic disk; (4) Zn disks; (5) Pt disk; (6) K-type thermocouple controlling the furnace; and (7) K-type thermocouple measuring sample temperature.

sketch of the sample position can be seen in Figure 2. The tips of the three thermocouples are fed through three small holes in the Ag tube. The two thermocouples located within the wall of the Ag tube are used to control the two heating zones of the furnace. The third thermocouple, which is in contact with the sample, is used for measuring the sample temperature. A thin alumina disk below the sample avoids chemical contamination of the silica piston and reduces the heat transfer from the sample to the piston.

The stress is transmitted to the sample by a second silica piston. This piston is guided through a bore in the upper steel disk into the cold part of the viscometer. On the top of the piston rests a load, which is connected to the piston by a link made of steel and pyrophyllite. With this load the applied stress can be adjusted precisely. The load consists of Al, brass, and/or Pb disks, and can be varied between 100 and 1050 g. By means of three guide bars fixed on the top of the furnace, the load is centered on the silica piston. A steel plate at the top of the guide bars keeps them in a parallel orientation. The soft iron core of the displacement transducer is attached to the load. The transducer is fixed to the upper closure head. The transducer is a pressure-resistant, linear variable differential transducer (LVDT, Schaevitz 250 MHR-396) with a measuring range of 12 mm and a resolution of 0.1 μm. The upper closure head holds two ports for the lines of the LVDT and the inlet for the pressure medium. Enameled Cu wires are used to guide the connections for the LVDT through the ports.

The signal of the transducer as well as the temperatures measured by the three thermocouples are monitored by a scanning multimeter (Keithley DMM 195) and stored by a IBM compatible PC. A TurboPascal program calculates the viscosity from the measured deformation rate and displays the result in real time.

OPERATION OF THE VISCOMETER

Glass cylinders cored from glass blocks were used for the viscosity measurements. The dimensions of the cylinders ranged between 3–4 mm in diameter and 8–12 mm in length. The ends of the cylinder were cut and polished parallel. The initial diameter and length of the cylinder were determined with a micrometer (Mitutoyo, range: 0–25 mm) to a precision of ±0.001 mm. For the purpose of temperature calibration, Zn disks (∅ = 4 mm, thickness = 0.1 mm, purity 99.95%) were attached to both ends of the sample using a small amount (<1 mg) of mounting wax (Deibereit 502). Additional disks of Pt foil (∅6 mm, thickness = 0.05 mm) were inserted between sample and piston to protect the silica piston from contamination by the sample. After positioning the sample in the Ag tube within the furnace, the upper silica piston and the load were placed on the sample. The weight of the mass was determined at ambient pressure to ±100 mg. While operating the viscometer at a pressure higher than ambient, the buoyancy of the load increases due to the high density of the pressure medium. For example, by increasing the pressure from 0.1 MPa to 200 MPa, the density of Ar increases from 0.0015 g/cm^3 to 1.17 g/cm^3 at 50 °C. The density of Ar as a function of pressure was calculated after Siewert et al. (1998). The effective weight of the load is given by

$$W_P = W_R - \frac{W_R \cdot \rho_{AR}}{\rho_L} \quad (2)$$

where W_P and W_R are the weight of the load at experimental pressure and the weight at 0.01 MPa, respectively, ρ_{Ar} is the density of Argon at experimental pressure, and ρ_L is the average density of the load determined to ±0.01 g/cm^3. After inserting the viscometer into the IHPV, the vessel is pressurized up to the final pressure. The pressure is measured by a strain gauge manometer to a precision of ±50 bar. The heating of the sample is performed in three steps. In the first step the sample is heated with a ramp of 30 °C/min to 30 °C below the expected melting point of the Zn disks. The melting point of Zn was corrected for pressure using the data of Lees and Williamson (1965) and Akella et al. (1973). A second ramp of 4 °C/min is used until the melting of the Zn is detected by a sudden movement of the load. Subsequent heating increases T at a rate of 20 °C/min up to the temperature at which the first viscosity determination is performed.

At the beginning of the viscosity measurements, a period of ~30 minutes is required for thermal equilibration of the viscometer and the vessel. After the system reaches thermal equilibrium and the first viscosity value is obtained, the temperature

is changed in steps of 5–10 °C before the next measurement. Small changes in temperature require only short delays for thermal stabilization of the system (see Fig. 3). After several viscosity measurements at different temperatures, a previously established temperature is reestablished to check for any drift of the viscosity data. By this procedure up to 20 viscosity measurements at different temperatures were determined on the same sample without exceeding a total deformation of 40% from the initial length of the sample. After isobaric quenching the samples are removed from the viscometer and examined for regular deformation.

With the setup presented here, viscosity determinations are possible in the range $10^{8.5}$ to $10^{11.5}$ Pa·s. Measurement over this entire range necessitates a decrease (or increase) of the load and thus an interruption of the experiment. The effective range of viscosity that can be obtained in one single experiment covers 2.5 orders-of-magnitude.

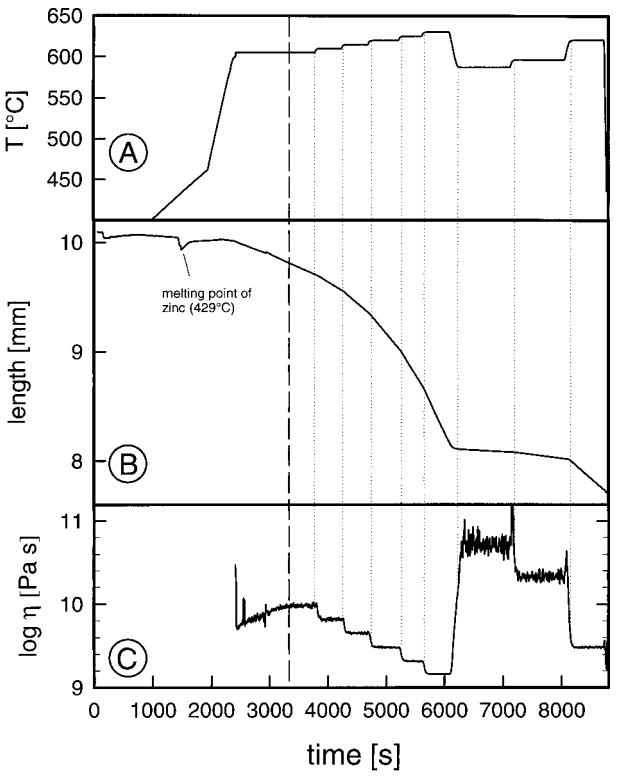

FIGURE 3. Evolution of run temperature (**A**), sample length (**B**), and calculated melt viscosity (**C**) with time for an experiment on the standard melt DGG1 at 200 MPa. The time interval for each viscosity calculation was 30 s. Because of this short time interval, the viscosity data at the lowest temperatures are quite noisy due to the resolution limit of the LVDT (deformation of the sample within 30 s = $8\Diamond10^{-3}$ mm). Viscosities presented in the subsequent figures are always the mean for each temperature. The plot demonstrates that during the high-pressure experiments at a constant temperature, no drift or sudden scatter occurs in the data. The dashed line indicates the time of thermal stabilization of the setup. The dotted lines represent times of temperature change.

SOURCES OF ERROR AND PRECISION OF MEASUREMENTS

Temperature

Of great importance for the quality of viscosity measurements is a precise measurement of the sample temperature. Small changes in temperature can produce large errors in viscosity. As described above, in every viscosity determination the melting point of Zn is determined giving a calibration value in the temperature range 419–432 °C (for 0.1–300 MPa). To prove that the calibration value thus obtained is transferable to the temperature of the viscosity measurements, separate calibration runs were carried out measuring the melting point of Al as a function of pressure (660–679 °C at 0.1–300 MPa; Lees and Willamsen 1965) and the α–β transition of quartz (573–652 °C at 0.1–300 MPa; Yoder 1950). In the whole *T*-range of calibration, the temperatures determined by phase transitions are 3–4 °C higher than those measured by the thermocouple at the sample position (no. 7 in Fig. 2). From these calibration runs we believe the maximum temperature uncertainty to be within ±2 °C. This is an excellent value for experiments in the IHPV.

The use of Zn disks on both sides of the sample provides a simple method to detect a thermal gradient along the sample because two clearly distinguishable melting events will be monitored by the transducer. The absence of a temperature gradient also can be recognized from the shape of the sample after the experiment. Any temperature gradient will result in an irregular shape of the sample.

Another possible source of error is determination of the effective load. The temperature is not known exactly at the load and might deviate from estimated value of 50 °C by ±30 °C. Great care was taken to prevent hot gas from escaping the furnace by keeping the outlets of the silica piston as narrow as possible. Furthermore, the upper part of the viscometer is shielded by a ceramic disk holding the upper silica piston (part no. 7 in Fig. 1).

We suggest that water cooling of the autoclave is sufficiently effective under the experimental conditions to hold the temperature of the load and the surrounding gas below 80 °C. However, the stated uncertainty in temperature has only a minor effect on the buoyancy of the load. The resulting error of the calculated viscosity is less than 1%.

Thermal expansion and deformation of the viscometer

In our setup, only one LVDT is used to monitor changes in the length of the sample during the experiment. Thus, contributions of thermal expansion and mechanical deformation of viscometer components might overlay the creep deformation of the sample, resulting in a incorrect determination of the deformation rate. This possible problem was checked by using rigid silica-glass cylinders at the sample position. Thermal expansion was recognized in the initial heating period. After the run temperature was reached and a subsequent delay of about 30 min, the thermal conditions were stable and the LVDT signal did not vary with time. Small temperature changes by ±10 °C followed by dwells of ~10 min (as in normal viscosity measurements) did not result in any detectable expansion of the

setup. Therefore, on the time scale of the viscosity experiment we expect stable conditions, which is also proved by the good reproducibility of the experiments.

Friction

Great care was taken to minimize friction of the moving parts. Friction will cause a reduction of the effective load and an overestimation of the viscosity. The absence of friction was proven for the experimental setup by the calibration measurements at 0.1 MPa (see below). Due to small forces by the applied loads, the deformation rates are small in high-viscosity measurements (e.g., $8 \cdot 10^{-9}$ m/s at a viscosity of 10^{11} Pa·s for a cylinder of 4 mm in diameter and maximal loads of 1000 g). For such small deformation rates, friction will result in a stick-slip behavior rather than in a continuously acting reduction of the load. Stick-slip behavior will be recognized by a strong scatter in the viscosity, which was not observed in the experiments (see Fig. 3). An additional indication of the minor importance of friction is given by the good reproducibility of viscosity data for standard glasses using different loads (see below).

Calibration of the viscometer

In a first set of experiments, the reliability of the setup was tested by measuring the viscosity of the DGG1 viscosity standard glass of the German Glass Technical Society (Deutsche Glastechnische Gesellschaft) at 0.1 MPa. In a second set, measurements on DGG1-melt were performed at a confining pressure of 200 MPa. The temperature range of the experiments was 581–668 °C. The load varied between 275–1087 g leading to a stress of $3.8–8.4 \times 10^5$ Pa. An example for the evolution of temperature, sample length, and calculated viscosity during an experiment with the DGG1 melt at a pressure of 200 MPa is presented in Figure 3.

To obtain a gradient-free temperature distribution along the sample, two different furnaces differing in the positions of the Kanthal windings were used at ambient and elevated pressure. At 0.1 MPa longer windings had to be used. The sample is placed in the middle between the two windings of the furnace. Due to convective heat transport at pressures beyond 50 MPa, the position of the windings were shifted toward the lower end of the furnace and the sample is placed at the end of the upper winding. The sample position within the viscometer is identical for both furnaces.

Within the investigated temperature range the measured viscosities can be fitted by an Arrhenius equation of the form:

$$\log \eta = a + b / T(\mathrm{K}) \quad (3)$$

The values for the parameters *a* and *b* of Equation 3 for DGG1-melt are given in Table 1. Figure 4 compares the viscosities from both data sets with the 0.1 MPa values derived from the recommended fit equation given for the viscosity of this melt (Meerlender 1974).

The agreement between recommended and measured viscosities is fairly good for the measurements at 0.1 MPa. The scatter in the data is always within ±0.08 log units, which is comparable to the error given by Neuville and Richet (1991) for their 1 atm parallel-plate viscometer. In the case of the high-pressure measurements (200 MPa) we obtained a pronounced shift of the viscosities toward higher values. The mean deviation from the recommended values is +0.45 log units. The reproducibility of the measurements was tested in several runs. Regardless of changes in sample length and diameter as well as changes of the applied stress, the reproducibility was always within ±0.15 log units.

It must be emphasized that the precision within one experiment is much better. Based on the reproducibility of viscosities determined at the same pressure and temperature, the precision is estimated to be ±0.05 log units.

Effect of pressure on melt viscosity

To elucidate a possible influence of pressure on the melt viscosity, additional calibration of the viscometer was carried out using Di_{100}-melt and $Ab_{55}Di_{45}$-melt (composition given in wt%: Di = $CaMgSi_2O_6$, Ab = $NaAlSi_3O_8$). For these melts, viscosities at 0.1 MPa and at high pressure are known from previ-

Table 1. Experimental results of the viscosity determinations

Composition of melt	*P* (MPa)	*T*–range (°C)	No. of viscosity determinations	Parameters for Eq. 3		
				a	*b* (·10⁴)	r^2
DGG1	0.1	583–638	22	–18.19	2.440	0.998
	50	590–670	3	–22.316	2.819	0.995
	100	590–670	5	–21.592	2.758	0.991
	200	585–629	15	–21.07	2.725	0.993
	300	590–670	3	–28.312	3.371	0.995
Di_{100}	0.1	713–785	8	–38.87	5.058	0.998
	50	751–770	4	–37.86	4.954	0.998
	100	751–770	5	–39.82	5.168	0.996
	200	750–793	15	–38.45	5.058	0.998
	300	751–770	3	–44.26	5.671	0.998
$Ab_{55}Di_{45}$	200	709–754	19	–23.82	3.382	0.978
$Qz_{33}Ab_{33}An_{33}$	50	889	1	–	–	–
anhydrous	100	889	1	–	–	–
	200	854–895	8	–22.32	3.795	0.998
	300	889	1	–	–	–
$Qz_{33}Ab_{33}An_{33}$3.80 wt% H_2O	200	495–568	19	–14.31	1.955	0.990

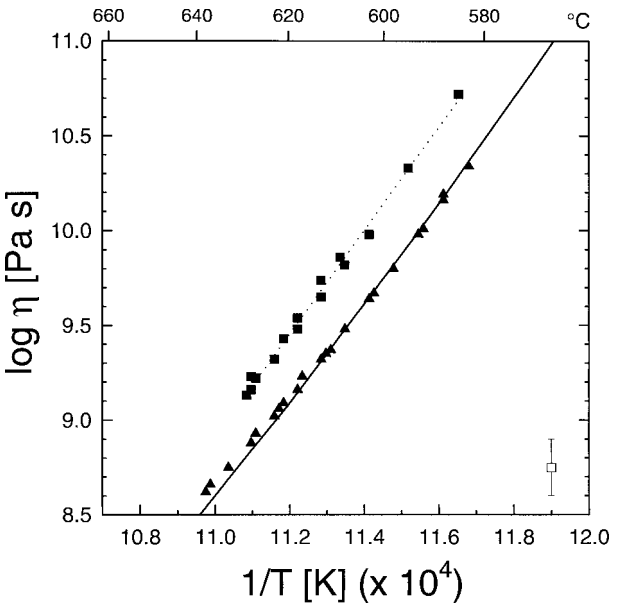

FIGURE 4. Viscosity of standard DGG1-melt determined at 0.1 MPa (triangles) and 200 MPa (squares). The solid line represents the values recommended by the Deutsche Glastechnische Gesellschaft, the dotted line is a fit after Equation 3 to the 200 MPa data.

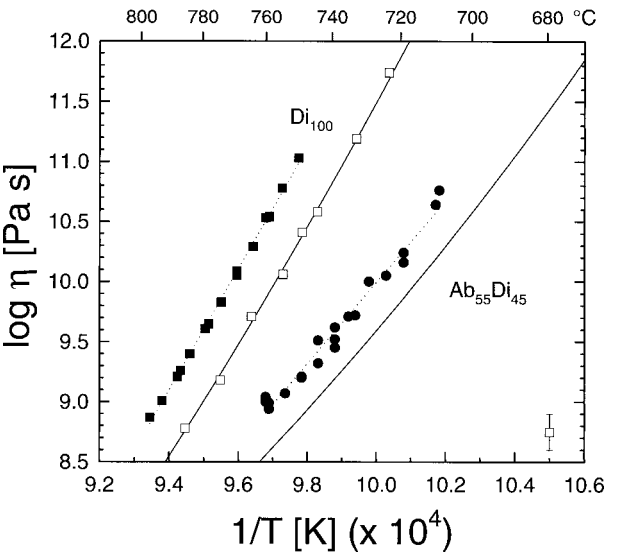

FIGURE 5. The viscosity of Di_{100}-melt (filled squares) and $Ab_{55}Di_{45}$-melt (filled circles) measured at 200 MPa. The low-pressure viscosities for Di_{100}-melt (hollow squares) were determined with the parallel plate viscometer described by Neuville and Richet (1991). Solid lines are fits to 0.1 MPa viscosities taken from literature [for Di_{100}-melt: Tauber and Arndt (1986); for $Ab_{55}Di_{45}$-melt: Tauber (1987)], dotted lines represent fits after Equation 3 to 200 MPa viscosities.

ous studies (Tauber 1987; Tauber and Arndt 1986; Brearley et al. 1986). In the case of the Di_{100}-melt, additional measurements at 0.1 MPa were performed using the parallel plate viscometer described by Neuville and Richet (1991).

Figure 5 compares the experimental results of the runs at 200 MPa and 0.1 MPa with the literature data for 0.1 MPa. The parameters for fits to Equation 3 are given in Table 1. As in the case of the DGG1-melt, the high-pressure viscosities are shifted toward higher values. In the case of the Di_{100}-melt, the observed deviation relative to the 0.1 MPa values is +0.6 log units. For the $Ab_{55}Di_{45}$-melt the deviation is only +0.3 log units. The strong deviations from the 0.1 MPa data are not expected from the published data on the pressure dependence of the viscosity of these melts (Brearley et al. 1986). However, it should be noted that for the temperature range of this study, no viscosity data obtained at high pressure are available.

To clarify the pressure dependence of the viscosity, two runs in which the pressure was varied systematically between 50 and 300 MPa were performed on DGG1-melt and on the Di_{100}-melt. The temperature range of the measurements was 590–617 °C for DGG1 and 751–770 °C for the Di_{100}-melt. Reestablishing previous *P-T*-conditions at the end of the experiment proves the reproducibility to be within the experimental error. The results are shown in Figure 6. Within the investigated pressure range the logarithm of the viscosities for both melts increase linearly with increasing pressure. For the Di_{100}-melt the viscosity increases by 0.23 log units/100 MPa at 751 °C and by 0.18 log units/100 MPa at 770 °C. For the DGG1-melt the pressure dependence is smaller in the same viscosity range. At 590 °C the viscosity increases by 0.17 log units/100 MPa and at 617 °C by 0.08 log units/100 MPa. Defining the activation energy of viscous flow as $E_a = 2.303*R*b$ (R = 8.314 J/mol·K), a systematic increase of E_a with increasing pressure is observed in experiments presented in Figure 6.

A linear extrapolation of the high-pressure data to 0.1 MPa leads to a deviation from the measured 0.1 MPa viscosities by $+0.15 \pm 0.07$ log units for both Di_{100} and DGG1 melts at the investigated temperatures. This deviation is close to the uncertainty of the method and, at present, it is not clear whether the apparent strong increase of viscosity at low pressure is an artifact of measurement or a real pressure effect on the melt viscosity. On the other hand, a curvature of the pressure dependence of viscosity has been observed for simple polymeric liquids (Matheson, 1966) implying that the strong *P* dependence of η at low pressures might be real.

At present, it is believed that the influence of pressure on the viscosity depends mainly on the degree of polymerization of the melt (e.g., Scarfe et al. 1987; Bottinga and Richet 1995). Defining the degree of polymerization of the melt as the ratio between non-bridging oxygen and tetrahedrally coordinated cations (NBO/T), it was shown by Brearley et al. (1986) for melts in the binary system Ab-Di that below NBO/T = 1 the viscosity increases with pressure. Beyond NBO/T = 1, increasing pressure causes a decrease of the viscosity. In the case of Di_{100}-melt with an NBO/T = 2, these findings are confirmed by our measurements. However, for the much more polymerized DGG1-melt with NBO/T = 0.75, viscosity also increases with pressure. This implies that the parameter NBO/T might be too

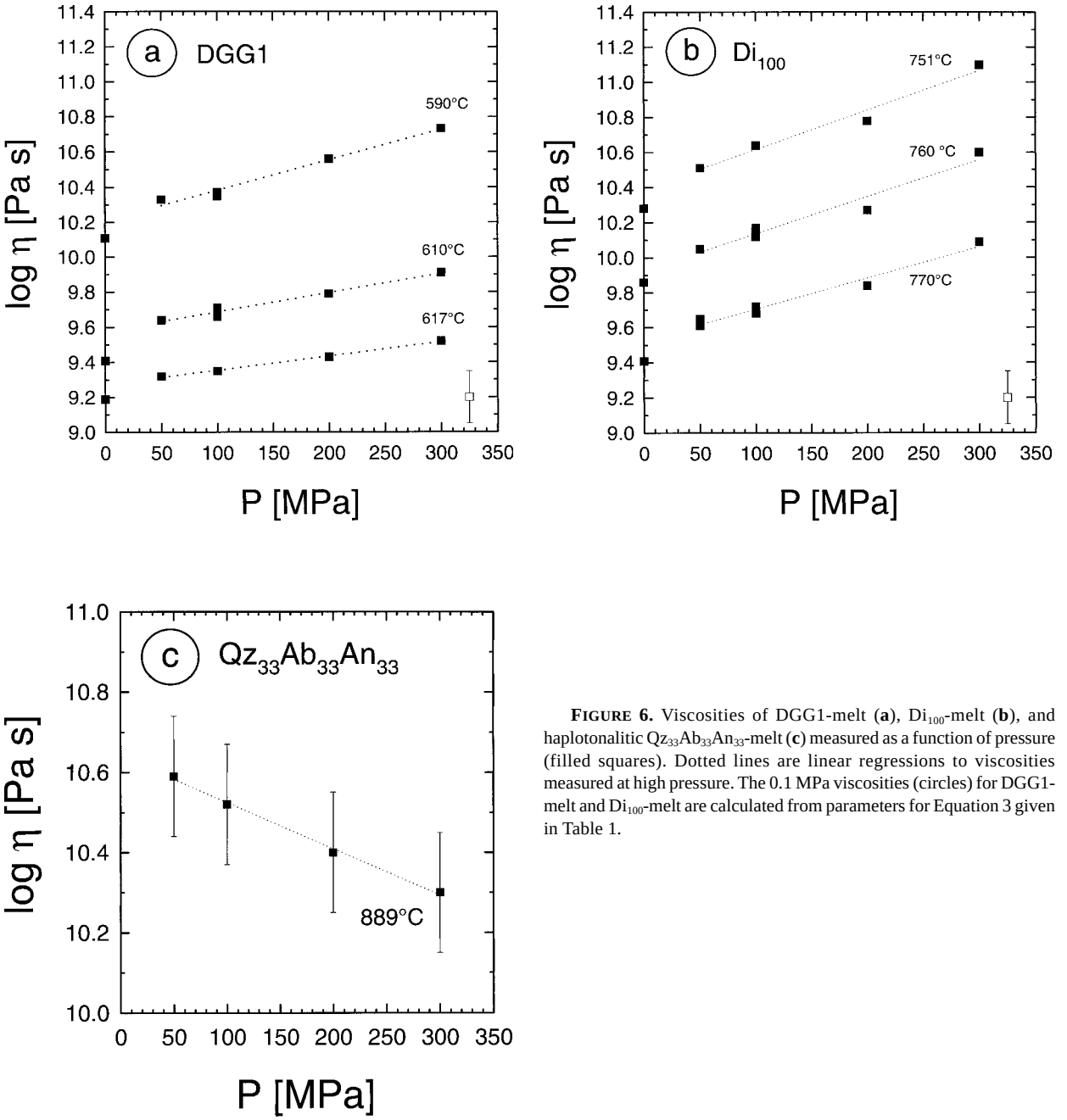

FIGURE 6. Viscosities of DGG1-melt (**a**), Di_{100}-melt (**b**), and haplotonalitic $Qz_{33}Ab_{33}An_{33}$-melt (**c**) measured as a function of pressure (filled squares). Dotted lines are linear regressions to viscosities measured at high pressure. The 0.1 MPa viscosities (circles) for DGG1-melt and Di_{100}-melt are calculated from parameters for Equation 3 given in Table 1.

crude to characterize the physical properties of a melt. There are also other effects such as, for example, the influence of the electron properties of the cations required for the charge balancing of Al^{3+} in tetrahedral coordination.

To clarify the observed effect of pressure on melt viscosity, additional measurements were performed on a fully polymerized melt of haplotonalitic composition (composition $Qz_{33}Ab_{33}An_{33}$, NBO/T = 0 [Qz = SiO_2, An = $CaAl_2Si_2O_8$]). For such a composition a decrease of the viscosity with increasing pressure is expected (Scarfe et al. 1987). This is confirmed by our experimental results shown in Figure 6c. At a temperature of 889 °C, the viscosity decreases within the investigated pressure range by 0.12 log units/100 MPa.

An independent control on the observed *P*-dependence of the viscosity can be obtained by a comparison to high-pressure DTA-measurements by Rosenhauer et al. (1979) on the influence of pressure on the glass transition temperature, T_g, of Di_{100}-melt. Rosenhauer et al. (1979) found that T_g increases by a factor of 3.7 °C/100 MPa within a pressure range of 700 MPa. Using the relationship $\log_{10}\eta = 11.3 - \log_{10}|q|$ (Scherer 1984) and the

quench rates reported by Rosenhauer et al. (1979) the viscosity of diopside melt at Tg is calculated to be $10^{11.8}$ Pa·s. The corresponding value of T_g extrapolated from our measurements at 0.1 MPa is 720 °C, which is almost identical to T_g obtained from viscosity by Rosenhauer et al. (1979). The slope of the isokom for $10^{11.8}$ Pa·s derived from the data of Rosenhauer et al. (1979) is in good agreement with the isokoms for 10^{11}, 10^{10}, and 10^9 Pa·s derived from the viscosity measurements in the present study (Fig. 7).

A further confirmation of the observed pressure dependence of the viscosity is given by Xue (1996) for a glass with a composition similar to DGG1. His high-*T* and high-*P* Brillouin scattering measurements indicate a pronounced increase of T_g with pressure.

APPLICATIONS TO HYDROUS MELTS

Besides investigating of the influence of pressure on viscosity, our new parallel-plate viscometer facilitates viscosity measurements on water-bearing melts because foaming is avoided. The method was used to determine the viscosity of a hydrous haplotonalitic melt (anhydrous composition: $Qz_{33}Ab_{33}An_{33}$). A hydrous glass cylinder containing 3.80 wt% H_20 was prepared as described by Schulze et al. (1996). The water contents of each end of the glass cylinders was determined using Karl-Fischer-titration (for the analytical technique see Behrens et al. 1996). The experiment was carried out at 200 MPa in the temperature range 495–568 °C. Viscosities were measured twice at selected temperatures to check for a drift in the values. No shift in the viscosity data with experimental duration was observed, indicating stable measurement conditions (Fig. 8).

After the experiment, the water content of the sample was measured with near-infrared-micro-spectroscopy on a thin polished disk (thickness: 500 μm) cut lengthwise from the deformed glass cylinder. To determine the concentrations of OH groups and of H_2O molecules, the combination bands at 4500 and 5200 cm^{-1}, respectively, were used. A small slit was used as an aperture in the microscope resulting in a lateral resolution of about 30 mm. [For further details on the spectroscopic method see Behrens et al. (1996)]. Within the length scale of the aperture, no gradients in the water content could be observed at the surface of the sample proving that water loss was negligible in the experiments.

The viscosity data for the hydrous melt are shown together with the data for the anhydrous melt in Figure 8. The measurements demonstrate that with the addition of water to the anhydrous haplotonalitic melt, the viscosity-temperature relationship is shifted toward lower temperatures. For instance, at a viscosity of $10^{10.5}$ Pa·s, the temperature is reduced by 369 °C (from 883 to 515 °C). The temperature-viscosity relationship is approximately Arrhenian for both melts in the investigated range of viscosities. The activation energy, E_a, decreases from 727 kJ/mol for the anhydrous melt to 374 kJ/mol for the hydrous melt.

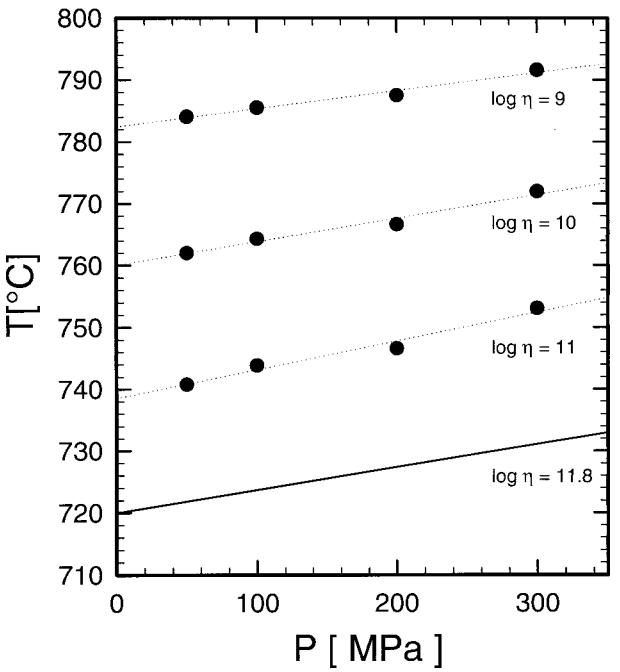

FIGURE 7. Isokoms for the viscosity of diopside melt. Solid line: Isokom for $10^{11.8}$ Pa·s representing the viscosity at the glass transition temperature T_g. The viscosity at Tg was calculated using the relationship $\log_{10} h = 11.3\text{-}\log |q|$ (Scherer 1984) The quenchrate |q| (25 °C/min) and the slope of the isokom (+3.7 °C/100 MPa) was taken from Rosenhauer et al. (1979). The dotted lines represent isokomes for 10^{11}, 10^{10}, and 10^9 Pa·s fitted to the viscosities calculated from the experimental results of this study (circles).

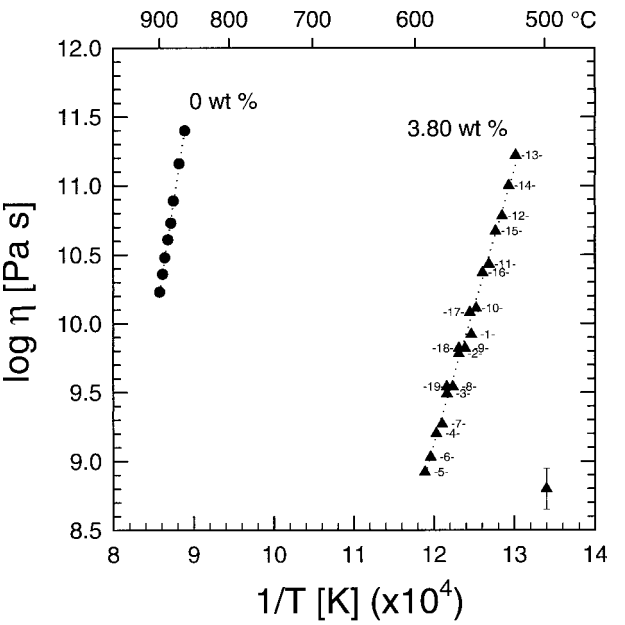

FIGURE 8. Viscosities of dry (circles) and hydrous (triangles) haplotonalitic melt. Numbers at the data points of hydrous melt indicate order of measurements.

The lowering of melt viscosity by addition of water is similar for the haplotonalitic melt and a leucogranitic melt for which the temperature-viscosity relationship was calculated using the model of Hess and Dingwell (1996). For the leucogranitic melt (NBO/T = 0 for anhydrous melt) the shift in temperature–viscosity relationship for conditions as noted above (3.8 wt% H_2O, $\log \eta = 10^{10.5}$ Pa·s) is calculated to be 412 °C.

In contrast, a more pronounced difference is observed when comparing our experimental results for the haplotonalitic melts to a synthetic iron free andesitic melt studied by Richet et al. (1996) using creep deformation at ambient pressure. For the andesitic melt, addition of 3.46 wt% H_2O reduces the temperature at which the melt viscosity is $10^{10.5}$ Pa·s by 290 °C (from 807 to 517 °C). Despite the small difference in water content for both melts, the difference might also be due to the fact that the anhydrous andesite is more depolymerized (NBO/T = 0.17) than the anhydrous tonalite (NBO/T = 0).

ACKNOWLEDGMENTS

We thank B.O. Mysen, A. Whittington, A. Withers, and an anonymous reviewer for their helpful comments. Thanks to F.M. Holtz for many helpful diskussions. The 0.1 MPa measurements on diopside melt were kindly performed by A. Whittington at the Institut de Physique du Globe de Paris. Technical assistance was provided by O. Dietrich. This study was supported by the Deutsche Forschungsgesellschaft and the European TMR project "In-situ hydrous melt properties (proposal no. ERBFMRX CT 960063)."

REFERENCES CITED

Akella, J., Ganguly, J., Grover, R., and Kennedy, G. (1973) Melting of lead and zinc to 60 kbar. Journal of Physics and Chemistry of Solids, 34, 631–636.

Baker, D.R. and Vaillancourt, J. (1995) The low viscosities of F + H_2O-bearing granitic melts and implications for melt extraction and transport. Earth and Planetary Science Letters, 132, 199–211.

Behrens, H., Romano, C., Nowak, M., Holtz, F., and Dingwell, D.B. (1996) Near-infrared spectroscopic determination of water species in glasses of the system $MAlSi_3O_8$ (M = Li, Na, K): an interlaboratory study. Chemical Geology, 128, 41–63

Bottinga, Y. and Richet, P. (1995) Silicate melts: The "anomalous" pressure dependence of the viscosity. Geochimica et Cosmochimica Acta, 59, 13, 2725–2731

Brearley, M., Dickinson, J.E., and Scarfe, C.M. (1986) Pressure dependence of melt viscosities on the join diopside-albite. Geochimica et Cosmochimica Acta, 50, 2563–2570.

Dingwell, D.B. (1987) Melt viscosities in the system $NaAlSi_3O_8$-H_2O-F_2O-1. In B.O. Mysen, Ed., Magmatic processes: physicochemical principles. The Geochemical Society, Special publication No.1, 423–433.

Dingwell, D.B. and Mysen, B.O. (1985) Effects of water on the viscosity of albite melt at high pressure: a preliminary investigation. Earth and Planetary Science Letters, 74, 266–274.

Dingwell, D.B., Romano, C., and Hess, K.-U. (1996) The effect of water on the viscosity of a haplogranitic melt under P-T-X conditions relevant to silicic volcanism. Contribution to mineralogy and petrology, 124, 19–28.

Dingwell, D.B., Hess, K.-U, and Romano, C. (1998) Extremely fluid behavior of hydrous peralkaline rhyolites. Earth and planetary science letters, 158, 31–38.

Dorfmann, A., Hess, K.-U., and Dingwell, D. (1996), Centrifuge-assisted falling-sphere viscometry. European Journal of Mineralogy, 8, 507–514.

Dorfmann, A., Dingwell, D.B., and Bagdassarov, N.S. (1997) A rotating autoclave for centrifuge studies: falling sphere viscometry. European Journal of Mineralogy, 9, 345–350.

Hess, K.-U. and Dingwell, D.B. (1996) Viscosities of hydrous leucogranitic melts: A non-arrhenian model. American Mineralogist, 81, 1297–1300.

Holtz, F., Roux, J., Ohlhorst, S., Behrens, and H., Schulze, F. (1999) The effects of silica and water on the viscosity of hydrous quartzofeldspathic melts. American Mineralogist, 84, 27–36.

Kushiro, I. (1978) Density and viscosity of hydrous calc-alkalic andesite magma at high pressure. Carnegie Institution of Washington Yearbook, 77, 675–677.

Lees, J. and Williamson, B.H.J. (1965) Combined very high pressure high temperature calibration of the tetrahedral anvil apparatus, fusion curves of zinc, aluminum, germanium, and silicon to 60 kilobars. Nature, 208, 278–279.

Matheson, A.J. (1966) Role of free volume in the pressure dependence of the viscosity of liquids. Journal of Chemical Physics, 44, 2, 695–699.

Meerlender, G. (1974) Viskositäts-Temperatur-Verhalten des Standardglases I der DGG. Glastechnische Berichte, 1, 1–3.

Neuville, D.R. and Richet, P. (1991) Viscosity and mixing in molten (Ca, Mg) pyroxenes and garnets. Geochimica et Cosmochimica Acta, 55, 1011–1019.

Persikov, E.S., Zharikov, V.A., Bukhtiyarov, P.G., and Polskoy, S.F. (1990) The effects of volatiles on the properties of magmatic melts. European Journal of Mineralogy, 2, 621–642.

Richet, P. and Bottinga, Y. (1995) Rheology and configurational entropy of silicate melts. Reviews in Mineralogy, 32, 67–93.

Richet, P., Lejeune, A.-M., Holtz, F., and Roux, J. (1996) Water and the viscosity of andesite melts. Chemical Geology, 128, 185–198.

Rosenhauer, M., Scarfe, C.M., and Virgo, D. (1979) Pressure dependence of the glass transition temperature in glasses of diopside, albite and sodium trisilicate composition. Carnegie Institution of Washington Yearbook, 78, 556–559.

Scaillet, B., Holtz, F., Pichavant, M., and Schmidt, M. (1996) Viscosity of himalayan leucogranites: Implications for mechanisms of granitic magma ascent. Journal of Geophysical Research, 101, No. B12, 27691–27699.

Scarfe, C.M., Mysen, B.O., and Virgo, D. (1987) Pressure dependence of the viscosity of silicate melts. In: Magmatic Processes: Physicochemical principles. Editor: B.O.Mysen. Geochemical Society, Special Publications, 1, 59–67.

Scherer, G.W. (1984) Use of the Adam-Gibbs equation in the analysis of structural relaxtion. Journal of the American Ceramic Society, 67, 504–511.

Schulze, F., Behrens, H., Holtz, F., Roux, J., and Johannes, W. (1996) The influence of H_2O on the viscosity of a haplogranitic melt. American Mineralogist, 81, 1155–1165.

Shaw, H.R. (1963) Obsidian-H_2O viscosities at 100 and 200 bars in the temperature range 700 to 900 ˚C. Journal of Geophysical Research, 68, 6337–6342.

——(1972) Viscosities of magmatic silicate liquids: an empirical method of prediction. American Journal of Science, 272, 870–893

Siewert, R., Büttner, H., and Rosenhauer, M. (1998) Experimental investigation of thermodynamic melting properties in the system NaCl-KCl at pressures of up to 7000 bar. Neues Jahrbuch für Mineralogie Abhandlungen, 172, 2/3, 259–278

Tauber, P. (1987) Viskositätsuntersuchungen im Modellsystem Anorthit-Albit-Diopsid. Ph-D. Thesis, Tübingen, 79 p.

Tauber, P. and Arndt, J. (1986) Viscosity-temperature relationship of liquid diopside. Physics of the Earth and Planetary Interiors, 43, 97–103.

White, B.S. and Montana, A. (1990) The effect of H_2O and CO_2 on the viscosity of sanidine liquid at high pressures. Journal of Geophysical Research, 95, 15683–15693,

Yoder, Jr., H.S. (1950) High-low quartz inversion up to 10,000 bars. Transactions, AGU, 31-6, 827–835.

MANUSCRIPT RECEIVED OCTOBER 26, 1998
MANUSCRIPT ACCEPTED JUNE 1, 1999
PAPER HANDLED BY WILLIAM A. BASSETT